The explanation of barrier height inhomogeneities in Au/n-Si Schottky barrier diodes with organic thin interfacial layer

İlke Taşçıoğlu,[a] Umut Aydemir, and Şemsettin Altındal
Department of Physics, Faculty of Arts and Sciences, Gazi University, 06500 Ankara, Turkey

(Received 22 May 2010; accepted 29 June 2010; published online 17 September 2010)

The forward bias current-voltage (I-V) characteristics of Au/n-Si Schottky barrier diodes (SBDs) with Zn doped poly(vinyl alcohol) (PVA:Zn) interfacial layer have been investigated in the wide temperature range of 80–400 K. The conventional Richardson plot of the $\ln(I_o/T^2)$ versus q/kT has two linear regions: the first region (200–400 K) and the second region (80–170 K). The values of activation energy (E_a) and Richardson constant (A^*) were obtained from this plot and especially the values of A^* are much lower than the known theoretical value for n-type Si. Also the value of E_a is almost equal to the half of the band gap energy of Si. Therefore, the Φ_{ap} versus $q/2kT$ plot was drawn to obtain the evidence of a Gaussian distribution (GD) of barrier heights (BHs) and it shows two linear region similar to $\ln(I_o)/T^2$ versus q/kT plot. The analysis of I-V data based on thermionic emission of the Au/PVA:Zn/n-Si SBDs has revealed the existence of double GD with mean BH values ($\bar{\Phi}_{B0}$) of 1.06 eV and 0.86 eV with standard deviation (σ) of 0.110 eV and 0.087 V, respectively. Thus, we modified $\ln(I_o/T^2)-(q\sigma)^2/2(kT)^2$ versus q/kT plot for two temperature regions (200–400 K and 80–170 K) and it gives renewed mean BHs $\bar{\Phi}_{B0}$ values as 1.06 eV and 0.85 eV with Richardson constant (A^*) values 121 $A/cm^2\,K^2$ and 80.4 $A/cm^2\,K^2$, respectively. This obtained value of $A^*=121$ $A/cm^2\,K^2$ is very close to the known theoretical value of 120 $A/cm^2\,K^2$ for n-type Si. © *2010 American Institute of Physics*. [doi:10.1063/1.3468376]

I. INTRODUCTION

Metal-insulator (MIS)/polymer-semiconductor Schottky barrier diodes (SBDs) is different from the ideal case due to barrier height (BH) and organic interfacial layer inhomogenities at metal-semiconductor (MS) interface, the energy distribution of interface states (N_{ss}), series resistance (R_s) of device and device temperature. The insulator or organic interfacial layer in the MIS structure separates the metal and semiconductor and prevents the interface diffusion and reaction. The MIS type SBDs or structures have been extensively studied in the past five decades.[1–15] The formation of BH at MS interfaces are still unclear and continuously object of investigation.[1–10] The first method was parallel conduction model to explain barrier inhomogeneities. However it remains invalid because, according to this method, the current is conveyed with linear small patches of lower BH occurred in large area of uniform higher BH. Then, Tung and co-workers[1,11,12] proposed a new model for current-conduction mechanisms in inhomogeneous barrier of SBDs based on the pinch-off phenomenon and applied it on various SBDs successfully. Palm *et al.*[13] have shown direct images of Schottky BH (SBH) fluctuations in Au–Si contacts by using ballistic electron emission microscopy and presented them with a Gaussian distribution (GD). The analysis of current-voltage (I-V) characteristics is the most commonly used and also it is an easy method for explanation of barrier inhomogeneities in SBDs and the evaluation of I-V results only at room temperature does not give detailed information about the nature of barrier formation at MS interface and current conduction mechanisms. On the other hand, the temperature dependence of I-V characteristics in the wide temperature range allows us to understand different aspects of the nature of barrier formation and current conduction mechanisms.

Many types of distribution functions have been used to describe BH inhomogenities.[7–17] Among them, the most preferred method is GD which explains most of the abnormal electrical characteristics of SBDs at low and high temperatures. Besides, the main electrical parameters of SBDs should have values nearby stable over a wide temperature range for reliability and usefulness in the integrated circuits or other applications.[18] Recently, the nature and origin of the temperature dependence of BH and ideality factor has been explained on the basis of thermionic emission diffusion (TED) theory with GD of BHs, which reveals an abnormal decrease in the BH and increase in the ideality with decreasing temperature, in the literature.[1–14] The physical underlying reason of BH formation is likely to be a function of the atomic interface structures, and the atomic inhomogenities at MS interface caused by grain boundaries, multiple phases, facets, defects, and mixture of different phases. Therefore, the current across the MS contact can be directly affected by the presence of BH inhomogenities.[1,19]

In recent years, the MS structures with organic interfacial layer are important research tools in the characterization of new semiconductor materials and the fabrication of these structures plays a crucial role in constructing some useful device technologies.[20–23] Electrical properties of MS devices obtained using a thin organic thin interfacial layer have been studied as photovoltaic cells, photodiodes, SBDs, field effect transistors, light emitting diodes, etc., by a great number of authors.[22–26] Kampen *et al.*[26] have presented that SBDs

[a]Electronic mail: ilketascioglu@gmail.com.

modified with organic thin interfacial layer on inorganic semiconductor could increase or decrease the effective Schottky barrier. This organic thin film such as polypyrrole, poly(vinyl alcohol) (PVA), polyaniline, poly (alkylthiophene), polyophene, poly (3-hexylthiophene), and plythiophene inserted at MS interface also influences the interface states, modifies some characteristics of these devices and converts MS diodes to metal-interfacial layer-semiconductor (MIS) type diodes.[3,27] The organic/inorganic semiconductor structures can be sensitive probe useful in establishing process for minimizing interface states, surface damage, dislocations, and contaminations that may ultimately increase the quality of the devices fabricated using the semiconductor. One of the main advantages of using organic materials is their production in large quantities by simple techniques such as spin coating, electrospinning methods which lower the production cost significantly, high electrical conductivity, and good environmental stability under ambient conditions compared with inorganic ones.[28] Another advantage of the polymers is that they do not need surfaces with regularity at the atomic level unlike inorganic semiconductors. There are different experimental and theoretically studies dealing with inorganic semiconductor devices by using polymers.[28–32]

In this respect, especially PVA nanofabrics have attracted much attention in the past decade due to it is unique chemical and physical properties as well as industrial applications.[21,33–36] PVA is semicrystalline which has crystalline and amorphous regions and these two regions are well separated by portions of an intermediate degree of ordering and this enhances macromolecules, producing several crystalline and amorphous phases.[34] Normally PVA is a poor electrical conductor and it is very important to conductivity of the polymer in construction in SBDs. In order to improve electrical conductivity, PVA is doped with Zn and it improved the device performance that of our previous study.[21] Doping of PVA is formed charge transfer complex between metal and semiconductor interface and charge transport mechanisms should also be discussed. In addition, the doping process affects the chemical structure, crystallinity, and electrical conductivity of polymers.[35,36]

In the present paper, the forward bias *I-V* characteristics of Au/PVA:Zn/n-Si SBDs were studied in the wide temperature range of 80–400 K in order to explain the origin of anomalous behavior of BH and ideality factor and significant underestimation of the Richardson's constant. The temperature dependent barrier inhomogeneities were evaluated on the basis of TED theory with double GD of the SBH. This paper exhibits the discrepancies observed in experimental results based on double GD model due to the barrier inhomogeneities at MS interface.

II. EXPERIMENTAL DETAILS

The Au/PVA:Zn/n-Si SBDs were fabricated on n-type (phosphor doped) float zone (100) single crystal Si wafer. First, the wafer was cleaned with RCA cleaning procedure. High purity Au metal (5*N*) with a thickness of ~1500 Å was thermally evaporated onto the whole back side of Si wafer in a pressure about 10^{-6} Torr in high vacuum thermal evaporation system. In order to perform good Ohmic behavior, Si wafer was annealed at 450 °C in pressure of 10^{-6} Torr.

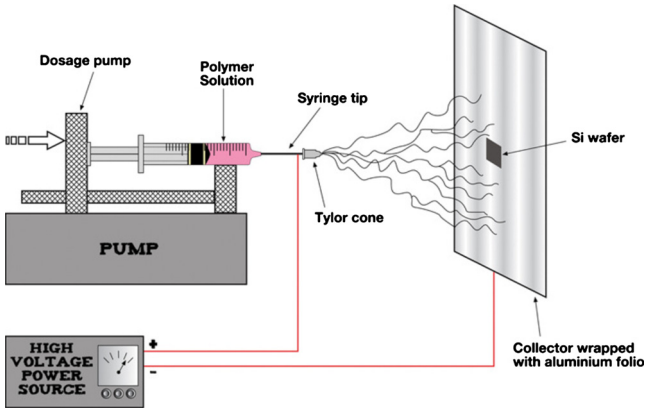

FIG. 1. (Color online) The schematic illustration of electrospinning system.

The PVA film was deposited on n-type Si substrate by electrospinning technique. A simple illustration of the electrospinning system was given in Fig. 1. 0.1 g of zinc acetate was mixed with 0.9 g of PVA, molecular weight=72 000 and 9 ml of deionised water. After vigorous stirring for 2 h at 50 °C, a viscous solution of PVA:Zn acetates was obtained. Using a peristaltic syringe pump, the precursor solution was delivered to a metal needle syringe (10 ml) with an inner diameter of 0.9 mm at a constant flow rate of 0.02 ml/h. The needle was connected to a high voltage power supply and positioned vertically on a clamp. A piece of flat aluminum foil was placed 15 cm below the tip of the needle to collect the nanofibers. Si wafer was placed on the aluminum foil. Upon applying a high voltage of 20 kV on the needle, a fluid jet was ejected from the tip. The solvent evaporated and a charged fiber was deposited onto the Si wafer as a nonwoven mat. After spinning process, circular dots of 1 mm diameter and 1500 Å thick high purity (5*N*) Au rectifying contacts were formed on the PVA:Zn surface of the wafer through a metal shadow mask in high vacuum system with pressure of about 10^{-6} Torr. In this way, Au/PVA:Zn/n-Si SBDs were fabricated for the electrical measurements and the electrode connections were made by silver paste. The schematic diagram of Au/PVA:Zn/n-Si SBD was given in Fig. 2.

I-V measurements were performed by means of a Keithley 2400 source-meter in the wide temperature range of 80–400 K using a temperature controller in Janis VPF-475

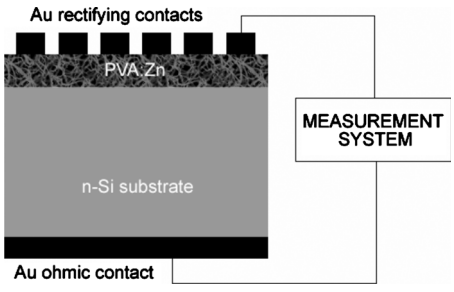

FIG. 2. The schematic diagram of Au/PVA:Zn/n-Si SBD.

cryostat with vacuum of $\sim 10^{-3}$ Torr. The sample temperature was always monitored by using a copper-constant an thermocouple close to the sample and measured with a dmm/scanner Keithley model 199 and Lake Shore model 321 autotunning temperature controllers with sensitivity better than $\pm$ 0.1 K. All measurements were carried out with the help of a microcomputer through an IEEE-488 ac/dc converter card.

III. RESULTS AND DISCUSSION

The relation between current and applied bias voltage for SBDs at forward bias voltage ($V \geq 3kT/q$), based on the thermionic emission (TE) theory is given by[37–39]

$$I = I_o \exp\left(\frac{qV}{\mathrm{n}kT}\right)\left[1 - \exp\left(\frac{-qV}{kT}\right)\right], \quad (1)$$

where, V is the applied bias voltage, q is the electronic charge, n is the ideality factor, k is the Boltzmann constant, T is the absolute temperature in kelvin, and I_o is the reverse saturation current extracted from the straight line intercept of ln I-V plot at zero bias and is given by,

$$I_0 = AA^*T^2 \exp\left(-\frac{q\Phi_{B0}}{kT}\right), \quad (2)$$

where A is the rectifier contact area, A^* is the effective Richardson constant (120 $\mathrm{A/cm^2\,K^2}$ for n-type Si), and Φ_{B0} is zero bias or apparent BH. The values of ideality factor n were obtained from the slope of the linear region of the forward bias ln I-V plot and can be calculated from Eq. (1) as

$$\mathrm{n} = \frac{q}{kT}\left[\frac{dV}{d(\ln I)}\right]. \quad (3)$$

The value of n is usually greater than unity (n=1) and the high value of n can be attributed to presence of an interlayer, particular distribution of N_{ss} at Si/PVA:Zn interface, series resistance and barrier inhomogenities.[5,38]

The ln I-V plots of Au/PVA:Zn/n-Si SBD presented in Fig. 3(a) depict increasingly linear behavior in the intermediate bias regions over several orders of current with decrease in temperature but the deviation of linearity stems from especially the effects of series resistance (R_s) and interfacial layer. In addition, it is observed from Fig. 3(a) that the I-V plots shift gradually toward higher bias voltages with decreasing temperature, which is in agreement with Eq. (1) governing the current transport across a Schottky diode by TED theory. We have performed least square fits of Eq. (1) to the linear part of the I-V plots. Using these fits, the experimental values of n and Φ_{B0} were determined from Eqs. (2) and (3), respectively, and given in Table I. As can be seen in Table I, we found n and Φ_{B0} values ranging from 1.25 eV and 0.871 eV (400 K) to 4.26 eV and 0.328 eV (80 K), respectively. Similar results have been presented by some authors for conventional Au/n-Si SBDs. Uğurel *et al.*[40] fabricated Au/n-Si/Al MS diode and reported the Φ_B and n with values of 0.73 eV and 1.44 at room temperature, respectively. Tataroğlu *et al.*[41] fabricated $\mathrm{Au/SiO_2/n\text{-}Si}$ MIS diode and presented the Φ_B and n values ranging from 0.624 eV and 2.898 (300 K) to 0.794 eV and 1.787 (400 K), respectively. Nuhoğlu *et al.*[42] reported a paper discussing annealing effect on Au/n-Si/Al MS diode and they calculated the Φ_B and n as 0.64 eV and 1.04 for unannealed sample, respectively. The large values of n can be attributed to the effects of the bias voltage drop across the interfacial layer, the particular distribution of interface states located at interfacial layer/semiconductor interface and fluctuations of BH at the MS interface.[2,5,19]

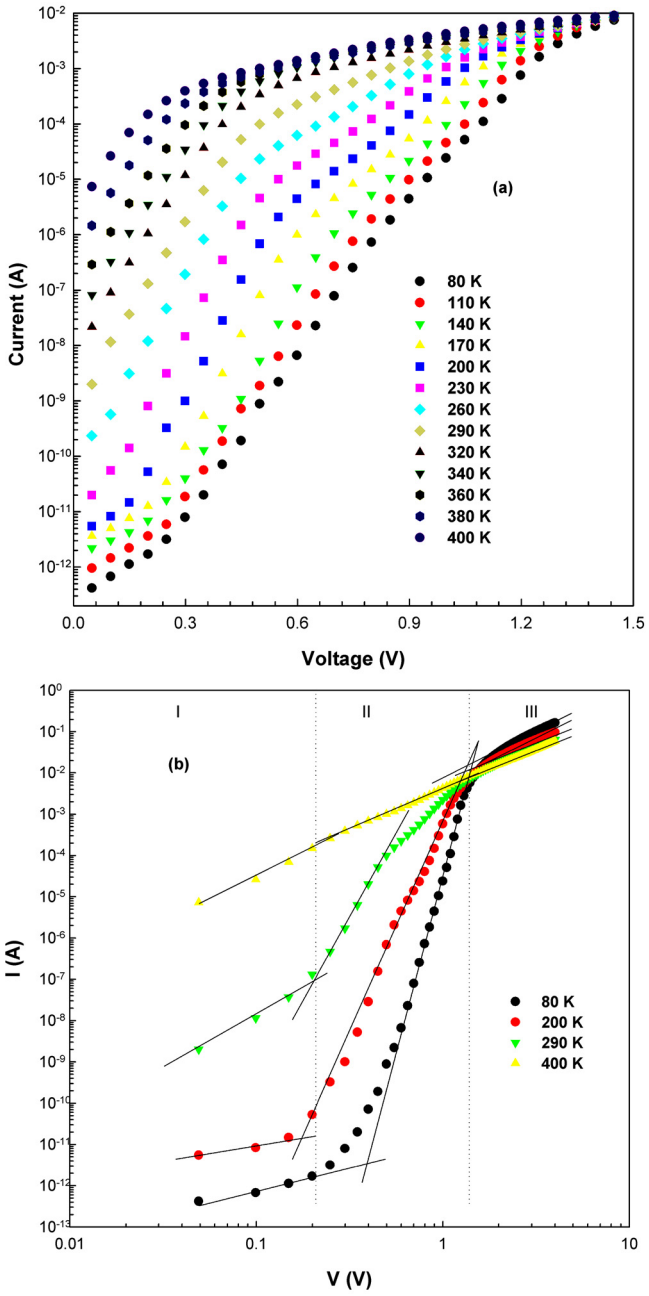

FIG. 3. (Color online) The forward bias (a) semi-logarithmic and (b) double-logarithmic I-V characteristics of Au/PVA:Zn/n-Si SBD at various temperature.

In order to explain current conduction mechanisms such as TE theory, space charge limited current (SCLC) mechanism and trap-charge limited current (TCLC), the forward bias double logarithmic plots of the I-V characteristics for Au/PVA:Zn/n-Si SBD were drawn and given in Fig. 3(b). As can be seen in Fig. 3(b), the forward bias ln(I)-ln(V) plots have three distinct linear regions with different slopes for

TABLE I. The electrical parameters obtained from *I-V* characteristics of Au/PVA:Zn/Si at various temperature.

T (K)	I_0 (A)	n	Φ_{B0} (eV)
80	1.45×10^{-17}	4.26	0.328
110	3.42×10^{-16}	3.44	0.427
140	1.00×10^{-15}	2.67	0.536
170	6.72×10^{-15}	2.09	0.628
200	9.65×10^{-14}	1.85	0.699
230	2.44×10^{-12}	1.73	0.745
260	3.51×10^{-11}	1.53	0.788
290	6.06×10^{-10}	1.46	0.813
320	6.49×10^{-9}	1.41	0.837
340	2.56×10^{-8}	1.37	0.853
360	9.14×10^{-8}	1.31	0.867
380	4.96×10^{-7}	1.29	0.869
400	1.63×10^{-6}	1.25	0.871

various temperatures, indicating different conduction mechanisms. In general, the double logarithmic *I-V* plots with a slope equal to or larger than two suggest the possibility of the SCLC mechanism at the intermediate ($\sim$0.3 V$\leq V<$1 V) and high bias voltage ($V\geq$1 V) regions.[20,43] At low bias voltage region ($V<$0.3 V) and especially low temperatures, the plots with slopes about unity show an Ohmic behavior. At the intermediate bias voltage region, where the slopes of the plots are larger than two, such behavior of the plot can be evaluated as an indication of TCLC mechanism with an exponent trap distribution. At high bias voltage region, the plots with slopes about 2 show SCLC mechanism for Au/PVA:Zn/n-Si SBD. As a result, it can be said that at high temperatures, the TE theory may dominate rather than the other current transport mechanisms.[20,43,44]

The n and Φ_{B0} plots as a function of temperature were presented in Fig. 4. As can be seen in Fig. 4, while the n increases, Φ_{B0} decreases with decreasing temperature. This increase in n is slow at high temperatures (230–400 K) and then this increase becomes more noticeable at low temperatures ($T\leq$230 K). On the other hand, while the Φ_{B0} decreases slowly from 400 to 260 K, this decrease is very steep down to 80 K. Such temperature dependence is obvious disagreement with the reported negative temperature coefficient of the BH or energy band gap of semiconductor.[37,39] Since, current transport across the SBD is temperature activated process, electrons at low temperatures are able to surmount lower barriers and thus, the current transport will be dominated by current flowing through the patches of lower BHs and as the temperature increases, more and more electrons have sufficient energy to surmount the higher barriers.[8–12,45–47] As a result, the dominant BH will increase with the temperature and applied bias voltage. An apparent increase in the n and a decrease in the BH at low temperatures are originated by some effects such as inhomogenities of BH and interfacial layer at MS interface and non uniformity of the interface charges. This gives rise to such an extra current that the overall characteristics still remains consistent with the TE process.[46,48]

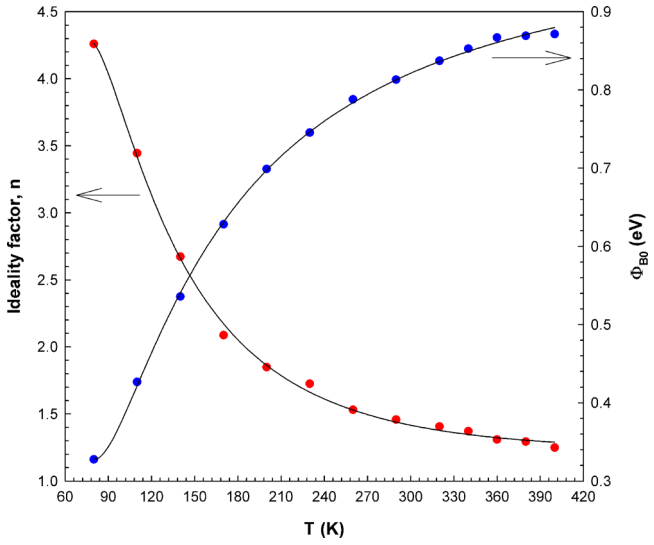

FIG. 4. (Color online) The Φ_{B0} and n plots of Au/PVA:Zn/n-Si SBD obtained from forward bias *I-V* data as a function of temperature.

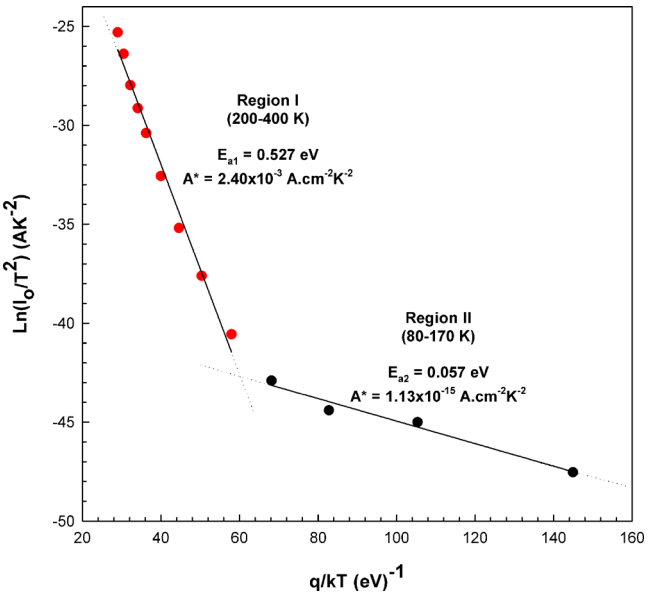

FIG. 5. (Color online) The Richardson plots of $\ln(I_o/T^2)$ vs q/kT for Au/PVA:Zn/n-Si SBD.

For the evaluation of the BH, Richardson plot of saturation current can be utilized and Eq. (2) can be rewritten as

$$\ln\left(\frac{I_0}{T^2}\right)=\ln(AA^*)-\frac{q\Phi_{B0}}{kT}. \tag{4}$$

A conventional activation energy or Richardson $\ln(I_o/T^2)$ versus q/kT plot was shown in Fig. 5. As can be seen in Fig. 5, the temperature dependence of $\ln(I_o/T^2)$ versus q/kT plot is found to be linear in two temperature region ranged from 80–170 K to 200–400 K. By means of fitting the experimental data at both temperature regions, the values of activation energy (E_a) and Richardson constant (A^*) were obtained from the slope of straight lines as 0.527 eV and 2.4×10^{-3} A/cm^2 K^2 for first region (200–400 K) and 0.057 eV and 1.13×10^{-15} A/cm^2 K^2 for second region (80–170 K), respectively. These Richardson constant values are much lower than the known theoretical value of 120 A/cm^2 K^2 for n-type Si.[37] The deviation of the Richardson plots may be

result of the spatially inhomogeneous BHs and potential fluctuations at the interface consisting of low and high barrier areas,[49–53] that is, the current through the diode will flow preferably through the lower barriers in the potential distributions and leads to increase in ideality factor at low temperature.

In order to explain observed deviation from classical TE theory, Tung and co-worker[1,11,12] have treated a system of discrete regions or "patches" of lower barrier imbedded in a higher background uniform barrier. Sullivan *et al.*[1] show that since the variation in BH may occur even at a scale much smaller than the depletion region width (W_D), the interaction between these patches should lead to pinch-off of the conduction path of small low barrier regions surrounded by regions with high BH. In this case, the current across the diode may be significantly affected by the existence of the BH inhomogenity and thus current through a low BH-patch depends on the height of the "saddle point" in front of it, and not the local BH at MS interfaces.[1,11,12,48–51] According to Tung's pinch-off approach,[11] there should be a linear correlation between obtained values of Φ_{B0} and n for various temperatures. Therefore, the plot of Φ_{B0} versus n was drawn for Au/PVA:Zn/n-Si SBD and given in Fig. 6(a). As can be clearly seen in the Fig. 6(a), there are two different linear regions which can be explained by the lateral inhomogeneities of the BHs.[4,8,12,50,54] In the first and second region, the extrapolation of the Φ_{B0} versus n plot, homogenous BHs values were obtained for Au/PVA:Zn/n-Si SBD as 0.95 eV and 0.77 eV in the case of n=1, respectively. The homogenous BH value obtained from the first region is closer to band gap energy of Si than the one obtained from the second region when they are compared with each other. These results indicate that the current transport is controlled by different mechanisms for separated temperature regions. For $T \geq 200$ K, the current transport is consistent with TE mechanism whereas it is consistent with thermionic field emission (TFE) mechanism across the diode for $T \leq 170$ K.[8,37,39]

In addition to the discussion of the main current transport mechanisms, the ideality factor is also analyzed by drawing $n(kT/q)$ versus (kT/q) plot in Fig. 6(b) showing the experimental and theoretical results of these plots. Figure 6(b) indicates that for the temperature values below 170 K TFE mechanism may be dominated for the current transport mechanism.[37,39] These experimental results confirm that current transport mechanism is not only controlled by TE mechanism but also controlled by other mechanisms for SBD. It can be emphasized from the experimental evidences above that the explanation of barrier inhomogeneities with double GD in a constant diode area is more suitable and more appropriate.

When Gaussian function is applied to Eq. (1) in constant diode area, the distribution of BH can be more precisely described by following equations:[2,3,8,50]

$$\Phi_{ap} = \bar{\Phi}_{B0} - \frac{q\sigma^2}{2kT}, \tag{5a}$$

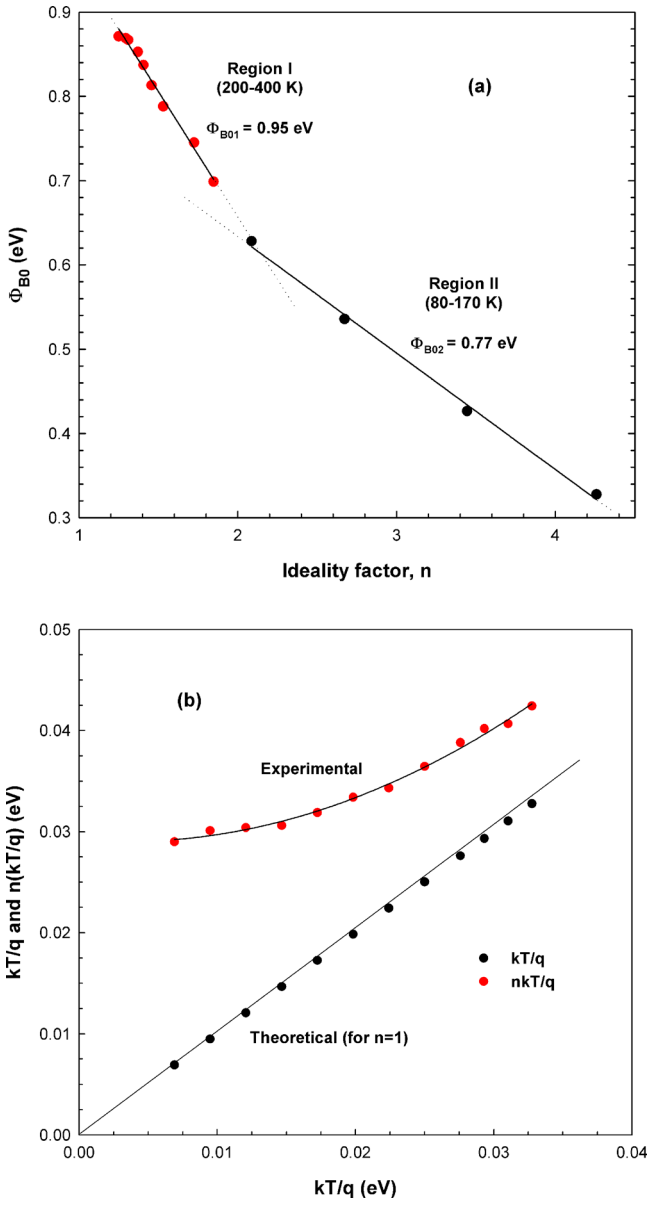

FIG. 6. (Color online) (a) Φ_{B0} vs n and (b) $n(kT/q)$ vs (kT/q) plots of Au/PVA:Zn/n-Si SBD at various temperatures.

$$\left(\frac{1}{n_{ap}} - 1\right) = \rho_2 - \frac{q\rho_3}{2kT}. \tag{5b}$$

Here, the terms of Φ_{B0} and n are changed with apparent BH (Φ_{ap}) and ideality factor n_{ap}, respectively. Also, the terms of ρ_2 and ρ_3 represent the voltage coefficients quantifying the voltage deformation of the BH distribution. According to Eq. (5a), the plot of Φ_{ap} versus $q/2kT$ should give a straight line whose the intercept point is equal to zero bias mean BH ($\bar{\Phi}_{B0}$) and the slope gives the standard deviation (σ) which is a measure of barrier homogeneity. The experimental Φ_{ap} versus $q/2kT$ and $n_{ap}^{-1} - 1$ versus $q/2kT$ plots were obtained with the help of Table I and given in Figs. 7(a) and 7(b). Figure 7(a) shows two straight lines which can be fit to determine $\bar{\Phi}_{B0}$ and σ values of Au/PVA:Zn/n-Si SBD for various temperatures. The intercepts and slopes of straight lines of Fig. 7(a) directly give the values of $\bar{\Phi}_{B0}$ and σ as 1.06 eV and

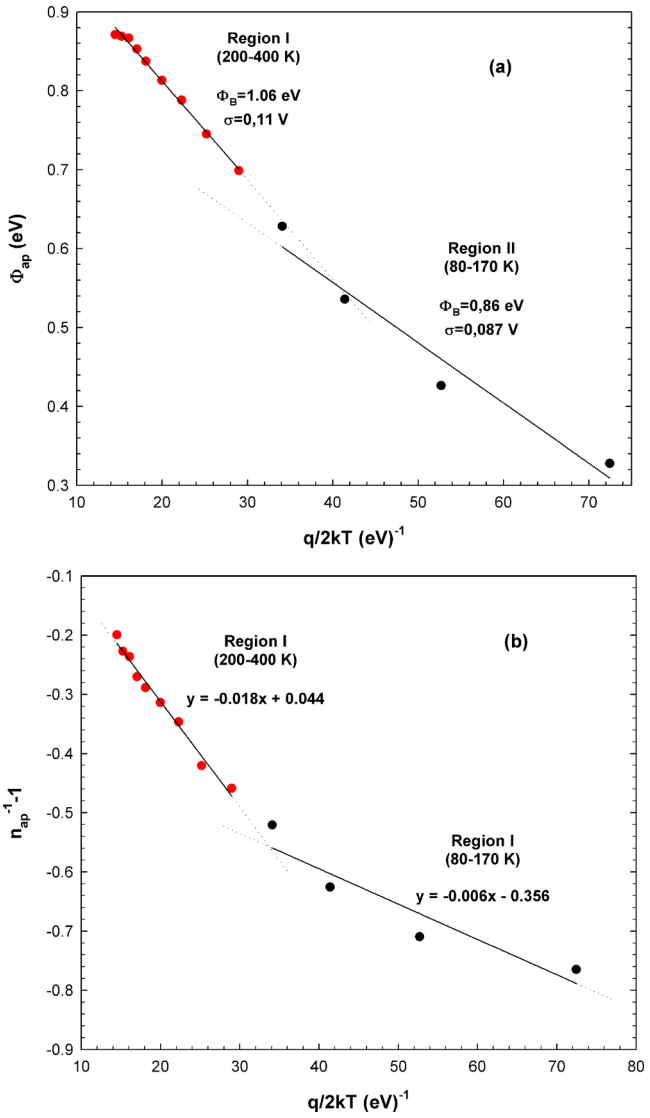

FIG. 7. (Color online) (a) Φ_{ap} vs $q/2kT$ and (b) $(n_{ap}^{-1}-1)$ vs $q/2kT$ plots of Au/PVA:Zn/n-Si SBD according to double GD of BHs.

0.110 V for first region and 0.86 eV and 0.087 V for second region, respectively. These observations indicate the double GD of BHs occurs in the studied contact area. On the other hand, as can be seen in Fig. 7(b), $(n_{ap}^{-1}-1)$ versus $q/2kT$ plots give two straight lines which correct the presence of double GD of BHs the diode area. Additionally, the linear behavior of this plot demonstrates that the ideality factor indeed express the voltage deformation of the GD of BHs. The values of ρ_2 and ρ_3 were obtained as 0.018 V and 0.044 V for first region and 0.006 V and 0.356 V for second region, respectively. We may conclude that the distribution of first region is wider and has relatively higher BH with smaller ρ_2 and larger ρ_3 voltage deformation coefficients rather than second region.

The conventional Richardson plot is modified by combining Eqs. (2) with Eqs. (5a) as follows:

$$\ln\left(\frac{I_0}{T^2}\right)-\frac{1}{2}\left(\frac{q\sigma}{kT}\right)^2=\ln(AA^*)-\frac{q\bar{\Phi}_{B0}}{kT}. \quad (6)$$

According to Eq. (6), the modified Richardson $[\ln(I_o/T^2)-(q\sigma)^2/2(kT)^2]$ versus q/kT plot given in Fig. 8 should give

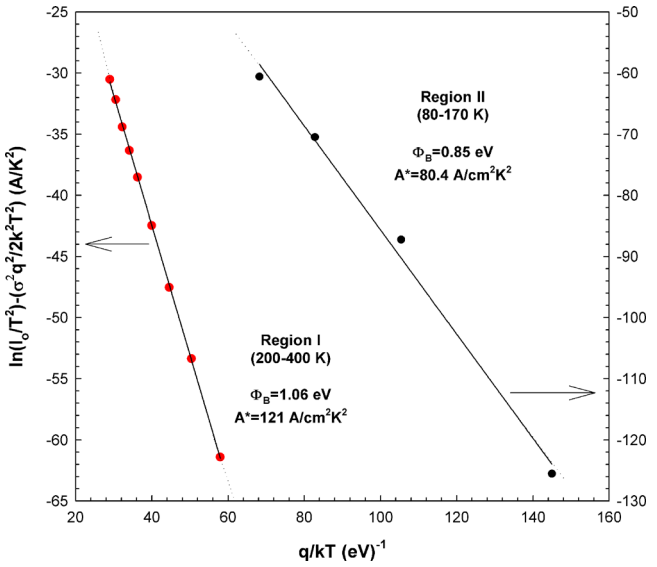

FIG. 8. (Color online) The modified Richardson $\ln(I_o/T^2)-(q\sigma)^2/2(kT)^2$ vs q/kT plot Au/PVA:Zn/n-Si SBD according to double GD of BHs.

a straight line with the slope directly yielding the mean BH $(\bar{\Phi}_{B0})$ and intercept $[\ln(AA^*)]$ at the ordinate determining A^* for a constant diode area (A). As it can be seen in Fig. 8, the temperature dependence of $\ln(I_o/T^2)-(q\sigma)^2/2(kT)^2$ versus q/kT plot is found to be linear in two temperature regions. By means of fitting the experimental data in both temperature regions, the values of $\bar{\Phi}_{B0}$ and A^* were obtained from the slope of straight lines as 1.06 eV and 121 $A/cm^2\,K^2$ for the first region and 0.85 eV and 80.4 $A/cm^2\,K^2$ for the second region, respectively. In particular, the obtained Richardson constant value of 121 $A/cm^2\,K^2$ found in the first region is very close to known theoretical value of 120 $A/cm^2\,K^2$ for n-type Si.[37] In addition, the obtained values of Φ_{B0} from Fig. 7(a) and Fig. 8 are in good agreement with each other. These results show that the temperature dependence of forward bias I-V characteristics of the Au/PVA:Zn/n-Si SBD can be successfully explained in terms of the TE mechanism with a double GD of BHs. Similar results have been reported in the literature.[6,8,10,44,47,55]

IV. CONCLUSIONS

The forward bias I-V characteristics of the Au/PVA:Zn/n-Si SBDs were measured in the wide temperature range of 80–400 K. Experimental results reveal an abnormal decrease in Φ_{B0} and an increase in the n with decreasing temperature, which stems from some effects such as inhomogenities of BH and interfacial layer at MS interface and nonuniformity of the interface charges. The values of A^* obtained from the conventional Richardson $\ln(I_o/T^2)$ versus q/kT plot are much lower than the known theoretical value for n-type Si. The analysis of I-V databased on TE of the Au/PVA:Zn/n-Si SBDs has revealed the existence of double GD with mean BH values $(\bar{\Phi}_{B0})$ of 1.06 and 0.86 eV with standard deviation (σ) of 0.110 V and 0.087 V, respectively. Then, the values of $\bar{\Phi}_{B0}$ and A^* were obtained from the modified Richardson $\ln(I_o/T^2)-(q\sigma)^2/2(kT)^2$ versus q/kT plot as 1.06 eV and

0.85 eV and 121 and 80.4 $A/cm^2 K^2$, respectively. In particular, the obtained Richardson constant with value of 121 $A/cm^2 K^2$ found in the first region (200–400 K) is very close to known theoretical value of 120 $A/cm^2 K^2$ for n-type Si. In addition, the obtained values of Φ_{B0} from Φ_{ap} versus $q/2kT$ and modified Richardson $\ln(I_o/T^2) - (q\sigma)^2/2(kT)^2$ versus q/kT plots are in good agreement with each other. Finally, it can be concluded that the temperature dependence of forward bias *I-V* characteristics of the Au/PVA:Zn/n-Si SBD can be successfully explained on the basis of the TE mechanism by assuming the presence of double GD of BHs.

[1] J. P. Sullivan, R. T. Tung, M. R. Pinto, and W. R. Graham, J. Appl. Phys. **70**, 7403 (1991).
[2] S. Chand and J. Kumar, Semicond. Sci. Technol. **12**, 899 (1997).
[3] S. Chand and J. Kumar, J. Appl. Phys. **82**, 5005 (1997).
[4] W. Mönch, J. Vac. Sci. Technol. B **17**, 1867 (1999).
[5] Ş. Aydoğan, M. Sağlam, and A. Türüt, Appl. Surf. Sci. **250**, 43 (2005).
[6] S. Huang and F. Lu, Appl. Surf. Sci. **252**, 4027 (2006).
[7] F. Iucolano, F. Roccaforte, F. Giannazzo, and V. Raineri, J. Appl. Phys. **102**, 113701 (2007).
[8] O. Pakma, N. Serin, T. Serin, and Ş. Altındal, J. Appl. Phys. **104**, 014501 (2008).
[9] J. Osvald, Microelectron. Eng. **86**, 117 (2009).
[10] V. Türüt, N. Yıldırım, and A. Türüt, "The theoretical and experimental study on double-Gaussian distribution in inhomogeneous barrier-height Schottky contacts," Microelectron. Eng. (to be published).
[11] R. T. Tung, Phys. Rev. B **45**, 13509 (1992).
[12] R. T. Tung, J. Appl. Phys. **88**, 7366 (2000).
[13] H. Palm, M. Arbes, and M. Schulz, Phys. Rev. Lett. **71**, 2224 (1993).
[14] I. Ohdomari and K. N. Tu, J. Appl. Phys. **51**, 3735 (1980).
[15] J. L. Freeouf, T. N. Jackson, S. E. Laux, and J. M. Woodall, Appl. Phys. Lett. **40**, 634 (1982).
[16] J. Osvald, Solid-State Electron. **35**, 1629 (1992).
[17] Z. J. Horvarth, Mater. Res. Soc. Symp. Proc. **260**, 367 (1992).
[18] S. Chand and J. Kumar, Appl. Phys. A: Mater. Sci. Process. **65**, 497 (1997).
[19] Ş. Altındal, H. Kanbur, A. Tataroğlu, and M. M. Bülbül, Physica B **399**, 146 (2007).
[20] Ö. Vural, Y. Şafak, Ş. Altındal, and A. Turut, Curr. Appl. Phys. **10**, 761 (2010).
[21] İ. Dökme, Ş. Altındal, T. Tunç, and I. Uslu, Microelectron. Reliab. **50**, 39 (2010).
[22] A. F. Özdemir, D. A. Aldemir, A. Kökce, and S. Altındal, Synth. Met. **159**, 1427 (2009).
[23] Y. S. Ocak, M. Kulakci, T. Kılıçoğlu, R. Turan, and K. Akkılıç, Synth. Met. **159**, 1603 (2009).
[24] O. Gullu and A. Turut, Sol. Energy Mater. Sol. Cells **92**, 1205 (2008).
[25] O. Güllü and A. Turut, J. Appl. Phys. **106**, 103717 (2009).
[26] T. Kampen, A. Schuller, D. R. T. Zahn, B. Biel, J. Ortega, R. Perez, and F. Flores, Appl. Surf. Sci. **234**, 341 (2004).
[27] R. Gupta, S. C. K. Misra, B. D. Malhotra, N. N. Beladakere, and S. Chandra, Appl. Phys. Lett. **58**, 51 (1991).
[28] F. Yakuphanoglu and S. Okur, Microelectron. Eng. **87**, 30 (2010).
[29] R. Singh, D. N. Srivastava, and R. A. Singh, Synth. Met. **121**, 1439 (2001).
[30] A. M. Farag, E. A. A. El-Shazly, M. Abdel Rafea, and A. Ibrahim, Sol. Energy Mater. Sol. Cells **93**, 1853 (2009).
[31] K. Akkılıç, M. E. Aydın, İ. Uzun, and T. Kılıçoğlu, Synth. Met. **156**, 958 (2006).
[32] M. Çakar, N. Yıldırım, Ş. Karataş, C. Temirci, and A. Turut, J. Appl. Phys. **100**, 074505 (2006).
[33] J. Zhang and F. Jiang, Chem. Phys. **289**, 243 (2003).
[34] S. M. Pawde, K. Deshmukh, and S. Parab, J. Appl. Polym. Sci. **109**, 1328 (2008).
[35] S.-A. Chen and Y. Fang, Synth. Met. **60**, 215 (1993).
[36] K. S. Kang, Y. Chen, H. K. Lim, K. Y. Cho, K. J. Han, and J. Kim, Thin Solid Films **517**, 6096 (2009).
[37] S. M. Sze and K. K. Ng, *Physics of Semiconductor Devices*, 3rd ed. (Wiley, New York, 2007.
[38] H. C. Card and E. H. Rhoderick, J. Phys. D: Appl. Phys. **4**, 1589 (1971).
[39] E. H. Rhoderick and R. H. Williams, *Metal Semiconductor Contacts* (Clarendon, Oxford, 1988).
[40] E. Uğurel, Ş. Aydoğan, K. Şerifoğlu, and A. Türüt, Microelectron. Eng. **85**, 2299 (2008).
[41] A. Tataroğlu and Ş. Altındal, J. Alloys Compd. **479**, 893 (2009).
[42] Ç. Nuhoğlu and Y. Gülen, Vacuum **84**, 812 (2010).
[43] Z. Ahmad and M. H. Sayyad, Physica E (Amsterdam) **41**, 631 (2009).
[44] H. Altuntaş, A. Bengi, U. Aydemir, T. Asar, S. S. Cetin, I. Kars, Ş. Altındal, and S. Özçelik, Mater. Sci. Semicond. Process. **12**, 224 (2009).
[45] M. K. Hudait, P. Venkateswarlu, and S. B. Krupanidhi, Solid-State Electron. **45**, 133 (2001).
[46] M. Biber, Physica B **325**, 138 (2003).
[47] F. E. Cimilli, M. Sağlam, H. Efeoğlu, and A. Türüt, Physica B **404**, 1558 (2009).
[48] S. Chand and J. Kumar, Semicond. Sci. Technol. **10**, 1680 (1995).
[49] S. Duman, B. Gurbulak, and A. Türüt, Appl. Surf. Sci. **253**, 3899 (2007).
[50] Ş. Karataş, Ş. Altındal, A. Türüt, and A. Özmen, Appl. Surf. Sci. **217**, 250 (2003).
[51] E. Dobročka and J. Osvald, Appl. Phys. Lett. **65**, 575 (1994).
[52] F. E. Jones, B. P. Wood, J. A. Myers, C. H. Daniels, and M. C. Lonergan, J. Appl. Phys. **86**, 6431 (1999).
[53] Zs. J. Horváth, Solid-State Electron. **39**, 176 (1996).
[54] R. F. Schmitsdorf, T. U. Kampen, and W. Mönch, Surf. Sci. **324**, 249 (1995).
[55] S. Chand and J. Kumar, Semicond. Sci. Technol. **11**, 1203 (1996).